OPTIMUM TAIL PLANE DESIGN FOR SAILPLANES

Kay Mayland
Technische Hochschule Darmstadt

SUMMARY

Classical drag equations in a modern version have been used to calculate the influence of tail modifications on the drag of a standard class sailplane. The profile drag which depends on the Reynolds number is included in the calculations. Minimum drag is compared with real drag for two lift coefficients.

Some results have no clear tendency but low tail area and relatively low tail aspect ratio give some advantages. Optimum and real lift ratios between wing and tail plane are compared for the original sailplane.

INTRODUCTION

Since the energy crisis in 1973 there is a lot of interest in reducing the trimmed drag of airplanes (Refs. 1-5). One contribution to the trimmed drag is the wing/tail interference drag. This interference drag had been interpreted as a component of the tail lift vector due to local downwash angle at the tail position. Sachs (Refs. 6, 7, 8, 9) has shown that this interpretation is not correct. The exact method is to calculate the interference drag with the aid of the downwash angle at downstream infinity. This new explanation corresponds to the well-known biplane theory of Prandtl and Munk (Ref. 10) which was also used in some new papers (Refs. 4, 11, 12). This theory in the modern version was used in this paper to show the relation between optimum and real load distributions between wing and tail.

Another purpose of this paper is to show the influence of tail plane design on total drag. It is important that the addition of the Reynolds number dependent profile drag has great influence on the optimum design.

All calculations are performed for a standard class sailplane.

SYMBOLS

Values are given in SI units.

AR	aspect ratio
b, b_t	wing span, tail span, m
C_D	drag coefficient
C_D^*	drag coefficient (tail profile drag + total induced drag)
C_L	lift coefficient
C_m	pitching moment coefficient
$\bar{c}$	mean aerodynamic chord, m
D	drag, N
g	acceleration of gravity, m/s^2
h, h_{wb}, h_t	distance in chord lengths from leading edge of wing to c.g., wing-body aerodynamic center, tail
k_{wb}, k_t	induced drag factor for wing-body, tail
L	lift, N
m	mass, kg
$\bar{q}$	dynamic pressure, N/m^2
Re	Reynolds number
S, S_t	wing and tail area, m^2
ε	downwash angle
ε_∞	downwash angle at downstream infinity
ε^*	downwash factor, $\varepsilon_\infty = \varepsilon^* k_{wb} C_{L_{wb}}$
μ	span ratio b_t/b
σ	interference factor

Subscripts:

min	minimum
o	zero lift
opt	optimum
t	tail
wb	wing-body

BASIC RELATIONS

The following fundamental relations were used, assuming that the aerodynamics are linear and that the dynamic pressure ratio is $\bar{q}_t/\bar{q} = 1$:

$$C_L = C_{L_{wb}} + C_{L_t} \frac{S_t}{S} \tag{1}$$

$$C_m = C_{mo_{wb}} + C_{L_{wb}} (h - h_{wb}) - C_{L_t} \frac{S_t}{S} (h_t - h) = 0 \tag{2}$$

$$C_m = C_{mo_{wb}} + C_L (h - h_{wb}) - C_{L_t} \frac{S_t}{S} (h_t - h_{wb}) = 0 \tag{2a}$$

$$C_D = C_{Do_{wb}} + k_{wb} C_{L_{wb}}^2 + \frac{S_t}{S} (C_{Do_t} + k_t C_{L_t}^2 + \varepsilon_\infty C_{L_t}) \tag{3}$$

The last term within the round brackets of the drag equation (3) is the wing/tail interference drag. The derivation was given by Sachs and shall not be repeated here. This interference drag is the product of the tail lift and the downwash angle at downstream infinity and corresponds to the one given by Prandtl but the new expression is much easier to use in calculations. The downwash angle at downstream infinity may be expressed as (Ref. 13)

$$\varepsilon_\infty = \varepsilon^* k_{wb} C_{L_{wb}} \qquad (\varepsilon^* = 0 - 3) \tag{4}$$

The downwash factor $\varepsilon^* = 1$ corresponds to a rectangular, $\varepsilon^* = 2$ to an elliptic and $\varepsilon^* = 3$ to a parabolic spanwise lift distribution of the wing.

Influence of Reynolds number

Wortmann (Ref. 14) has designed and measured a lot of excellent profiles for sailplanes. The wind tunnel test results are published in the "Stuttgarter Profilkatalog". Figure 1 shows some test results demonstrating the influence of Reynolds number on profile drag for several profiles. The solid lines are according to the relations used in this paper for calculating the influence of Reynolds number:

$$c_{Do_{wb}} = \frac{0.009}{Re_{wb}^{0.3}} \qquad \text{Re in millions} \qquad (5)$$

$$c_{Do_t} = \frac{0.007}{Re_t^{0.3}}$$

These relations are only valid for the above mentioned profiles and for a special Reynolds number range.

Real lift ratio

For balance in equilibrium flight ($C_m = 0$) equations (1) and (2) can be solved for the lift ratio between tail and wing

$$\left.\frac{L_t}{L_{wb}}\right|_{\substack{C_L=\text{const}\\ C_m=0}} = \frac{C_{L_t}\frac{S_t}{S}}{C_{L_{wb}}} = -\frac{\frac{C_{mo_{wb}}}{C_L} + (h - h_{wb})}{\frac{C_{mo_{wb}}}{C_L} + (h - h_{wb}) - (h_t - h_{wb})} \qquad (6)$$

This lift ratio depends on fixed quantities and on the parameters, total lift coefficient and c.g. position. It is possible to eliminate the c.g. position by considering the stability requirement. The static margin may be expressed as

$$\frac{\partial C_m}{\partial C_L} = (h - h_{wb}) - \frac{(C_{L_\alpha})_t}{C_{L_\alpha}}\frac{S_t}{S}(h_t - h_{wb})\left(1 - \frac{\partial \varepsilon}{\partial \alpha}\right) < 0 \qquad (7)$$

Solving equation (7) for $(h - h_{wb})$ and combining this with equation (6) gives the following equation:

$$\left.\frac{L_t}{L_{wb}}\right|_{\substack{C_L=\text{const}\\ C_m=0}} = -\frac{\frac{C_{mo_{wb}}}{C_L} + \frac{\partial C_m}{\partial C_L} + \frac{(C_{L_\alpha})_t}{C_{L_\alpha}}\frac{S_t}{S}(h-h_{wb})\left(1-\frac{\partial\varepsilon}{\partial\alpha}\right)}{\frac{C_{mo_{wb}}}{C_L} + \frac{\partial C_m}{\partial C_L} + \frac{(C_{L_\alpha})_t}{C_{L_\alpha}}\frac{S_t}{S}(h-h_{wb})\left(1-\frac{\partial\varepsilon}{\partial\alpha}\right) - (h_t-h_{wb})} \quad (8)$$

Regarding equation (8) it is possible to say that the real load distribution between tail and wing depends on several fixed values and on the parameters, stability margin and total lift coefficient.

Optimum load Distribution

Prandtl has published the optimum tail/wing lift ratio in his biplane theory (Ref. 10):

$$\left(\frac{L_t}{L_{wb}}\right)_{opt} = \frac{\mu-\sigma}{\frac{1}{\mu}-\sigma} \qquad \text{with } \mu = \frac{b_t}{b} \quad (9)$$

The interference factor σ has to be taken out of diagrams (Ref. 6). Therefore it is easier to use the following relations. Comparing Prandtl's equation for the interference drag

$$D_{Int} = \frac{2\,\sigma}{\pi\,\bar{q}}\frac{L_t\,L_{wb}}{b_t\,b} \quad (10)$$

with equation (3) it is possible to rewrite equation (9) as

$$\left(\frac{L_t}{L_{wb}}\right)_{opt} = \frac{1-\frac{\varepsilon^*}{2}}{\left(\frac{b}{b_t}\right)^2 - \frac{\varepsilon^*}{2}} \quad (11)$$

The optimum tail lift may be either positive or negative depending on the downwash factor ε^*. Only an elliptic spanwise lift distribution over the wing requires zero tail lift. The combination of equations (6) and (11) gives the optimum c.g. position

$$(h-h_{wb})_{opt} = -\frac{C_{mo_{wb}}}{C_L} + \frac{1-\frac{\varepsilon^*}{2}}{1+\left(\frac{b}{b_t}\right)^2 - \varepsilon^*}(h_t-h_{wb}) \quad (12)$$

and the optimum stability margin

$$\left(\frac{\partial C_m}{\partial C_L}\right)_{opt} = (h - h_{wb})_{opt} - \frac{(C_{L_\alpha})_t}{C_{L_\alpha}} \frac{S_t}{S} (h_t - h_{wb})\left(1 - \frac{\partial \varepsilon}{\partial \alpha}\right) \qquad (13)$$

The minimum induced drag was also given by Prandtl and may be rewritten in the following equation

$$C_{Di_{min}} = k_{wb} C_L^2 \left[1 - \frac{\left(1 - \frac{\varepsilon^*}{2}\right)^2}{1 + \left(\frac{b}{b_t}\right)^2 - \varepsilon^*}\right] \qquad (14)$$

The term in the brackets demonstrates the decreasing induced drag of the wing/tail combination compared with the wing alone.

NUMERICAL RESULTS

Optimum c.g. position

All calculations are performed with the data set of a typical standard class sailplane; see table 1.

The pilot of this airplane wants to know whether he can reach good performance by choosing the correct c.g. position. In figure 2 the equations (8) and (11) are evaluated. It is easy to see that the optimum load distribution depends on the downwash factor ε^* but not on the lift coefficient C_L while the real lift ratio has inversed dependencies. The downwash factor is normally not known exactly; therefore it is not easy to reach exact conclusions from figure 2. A more accurate way is to evaluate the equation (13); see figure 3. It is easy to see that the optimum stability margin for lift coefficients $C_L > 0.4$ is obtained by a normal (stable) c.g. position. This statement is valid for downwash factors between 1 and 2. Good performance for a wide range of lift coefficients will therefore be obtained by choosing a medium or forward c.g. position. Only high speed flight requires aft c.g. positions.

Tail modifications

While the pilot of a sailplane is interested in the optimum c.g. position, the sailplane designer is interested in the tail design to meet stability requirements and to achieve good performance. For a fixed wing geometry it is possible to vary two main parameters: tail area and tail span. It is important not to

evaluate the parameter variations only by regarding the total induced drag because the tail profile drag will also change. Therefore the criterion is the sum of both the total induced drag and the tail profile drag (equation 5)

$$C_D^* = C_{Di} + C_{Do_t} \frac{S_t}{S} \qquad (15)$$

The induced drag is calculated as in equation (3) with the lift coefficients obtained from the real load distribution (equation 8). The stability margin is assumed to be $\partial C_m/\partial C_L = -0.15$, and the downwash factor is assumed to be $\varepsilon^* = 1$. (The calculations were also performed for $\varepsilon^* = 2$; the tendencies correspond to $\varepsilon^* = 1$.) The real drag coefficient is compared with the theoretical minimum drag coefficient using equation (14) for the minimum induced drag.

In figure 4 this drag coefficient is plotted versus the tail span with constant tail m.a.c. for two lift coefficients. Parameter in this diagram is the tail profile drag at Re = 10^6. The minimum induced drag ($C_{Do_t} = 0$) is decreasing with increasing tail span but the higher profile drag due to increasing tail area is predominant. It is suitable to design the tail with the minimum possible area to satisfy stability requirements.

Assuming a minimum tail area of 1 m^2, another question is, what span or what AR_t is optimum? There are two effects:

- With increasing tail span the minimum induced drag of the complete sailplane is decreasing
- Increasing tail span means decreasing Reynolds number resulting in increasing tail profile drag.

In figure 5 it is shown that the superposition of these two effects results in no clear tendency. With increasing profile drag the Reynolds number effect becomes predominant. Assuming a tail profile drag coefficient of $C_{Do_t} = 0.01$ at $Re_t = 10^6$ a reduction of tail span from 2.4 m (original value) to perhaps 2.0 m will give some little advantages.

The differences between minimum and real drag coefficients are generally small; only low total lift coefficients ($C_L = 0.2$) require high tail downloads (see figure 2) resulting in greater differences.

Wing and tail modifications

The wing geometry is included in the variations. The only restrictions are now a wing span of 15 m and a total area (wing +

tail) of 11 m^2. To simplify the calculations it is assumed that wing and tail have the same profile drag at Re = 10^6. It is suitable to regard the drag or the drag areas directly rather than the drag coefficient:

$$\frac{D_o}{\bar{q}} = C_{Do}\, S = (C_{Do})_{Re=10^6} \left(\frac{S}{Re^{0.3}} + \frac{S_t}{Re_t^{0.3}}\right) \tag{16}$$

$$\frac{D_{i_{min}}}{\bar{q}} = k_{wb}\, C_L^2\, S \left[1 - \frac{(1 - \frac{\varepsilon^*}{2})^2}{1 + (\frac{b}{b_t})^2 - \varepsilon^*}\right]$$

$$= \left(\frac{m\, g}{\bar{q}\, b}\right)^2 \frac{1}{\pi} \left[1 - \frac{(1 - \frac{\varepsilon^*}{2})^2}{1 + (\frac{b}{b_t})^2 - \varepsilon^*}\right] \tag{17}$$

Figure 6 shows the total profile drag area (equation 16) plotted versus the ratio of tail area to total area. For normal tail aspect ratios between 3 and 6 the total profile drag will increase with increasing tail area due to decreasing medium Reynolds number of the total area.

The combination of equations (16) and (17) gives the minimum total drag D_{min} which is plotted versus the ratio of tail area to total area in figure 7. The trends are clear: the lowest possible drag is obtained with low ratios of tail area to total area.

CONCLUSIONS

The influences of c.g. position and of tail plane design on the performance of a standard class sailplane have been shown. One important result is that the optimum c.g. position is for a wide range of lift coefficients within the normal c.g. range. The calculations for the tail plane design have shown that the reduction of induced drag due to higher tail span is less important than the influence of profile drag. Low tail area and relatively low tail aspect ratio will give some advantages. It is remarkable that the best standard class sailplanes of today have a tail area of $S_t \approx 1$ m^2 and a tail aspect ratio of $AR_t \approx 5$ while older sailplanes have for example $S_t = 1.5$ m^2 and $AR_t = 6$.

REFERENCES

1. S.E. Goldstein and G.P. Combs: Trimmed drag and maximum flight efficiency of aft tail and canard configurations. AIAA Paper 74-69 (1974).

2. F.H. Lutze, Jr.: Trimmed drag considerations. J. Aircraft 14 (1977), pp. 544-546.

3. F.H. Lutze, Jr.: Reduction of trimmed drag. In: NASA CR-145 627 (1975), pp. 307-318.

4. E.E. Larrabee: Trim drag in the light of Munk's stagger theorem. In: NASA CR-145 627 (1975), pp. 319-329.

5. J. Roskam: Some comments on trim drag. In: NASA CR-145 627 (1975), pp. 295-305.

6. G. Sachs: Leitwerksauslegung und künstliche Stabilität. Dornier-Bericht 77/16 A (1977).

7. G. Sachs: Optimale Leitwerksauslegung für Flugzeuge künstlicher Stabilität. Zeitschrift für Flugwissenschaften Heft 1, 1978, pp. 1-10.

8. G. Sachs: Einfluß des Leitwerks auf die Flugleistungen. Institut für Flugtechnik der Technischen Hochschule Darmstadt, IFD-Bericht 2/77, 1977.

9. G. Sachs: Minimum Trimmed Drag and Optimum C.G. Position. J. Aircraft 15 (1978), pp. 456-459.

10. L. Prandtl: Tragflügeltheorie. 2. Mitteilung. Nachr. Ges. Wiss. Göttingen, Math.-phys. Kl. 1919, pp. 107-137.

11. E.V. Laitone: Ideal tail load for minimum aircraft drag. J. Aircraft 15 (1978), pp. 190-193.

12. McLaughlin: Calculations and comparison with an ideal minimum of trimmed drag for conventional and canard configurations having various levels of static stability. NASA-TN-D-8391, May 1977.

13. H. Schlichting und E. Truckenbrodt: Aerodynamik des Flugzeuges, 2. Band. Springer-Verlag, Berlin/Heidelberg/ New York 1969.

14. F.X. Wortmann and D. Althaus: Stuttgarter Profilkatalog, Institut für Aerodynamik, Universität Stuttgart, 1972.

15. F. Thomas: Grundlagen für den Entwurf von Segelflugzeugen. DFVLR-Bericht IB 154-78/8, November 1976.

TABLE 1.- DATA SET OF A TYPICAL SAILPLANE

[Reference 10]

Mass, kg	300
Wing:	
Span, m	15
Area, m^2	10
Mean aerodynamic chord, m	0.67
Aspect ratio	22.5
Pitching moment coefficient, zero lift	-0.1
Horizontal tail:	
Span, m	2.4
Area, m^2	1.0
Aspect ratio	5.76
Distance between wing and tail aerodynamic centers, m	3.85
Stability margin	-0.15

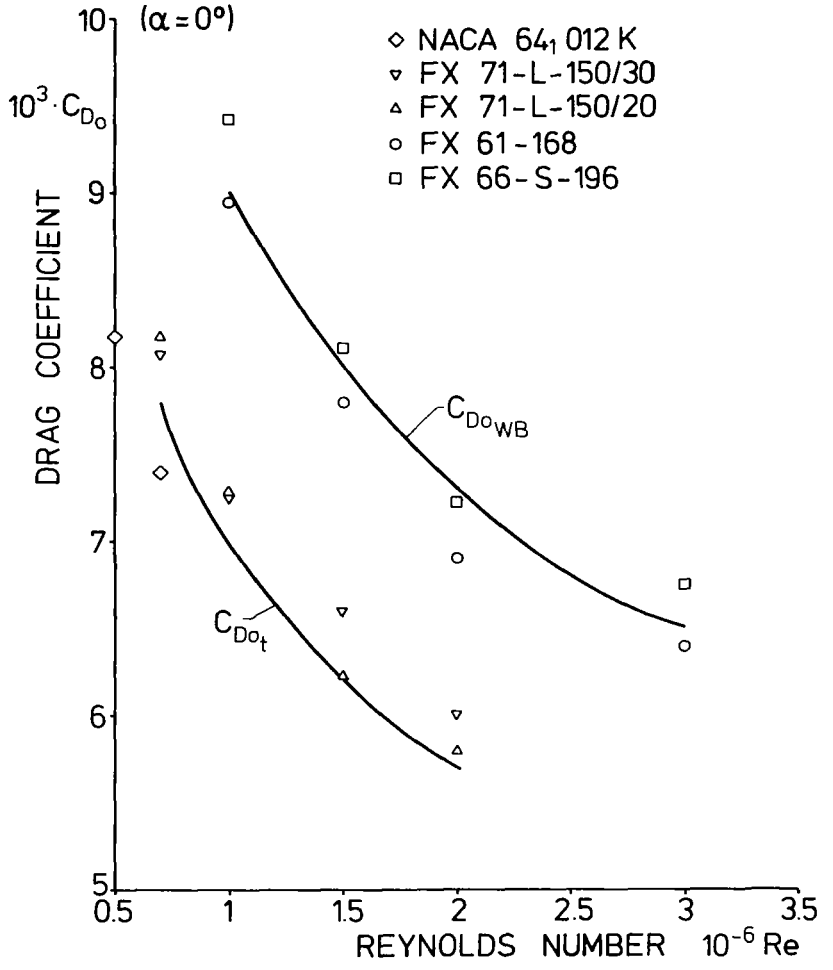

Fig. 1: Influence of Reynolds number on profile drag

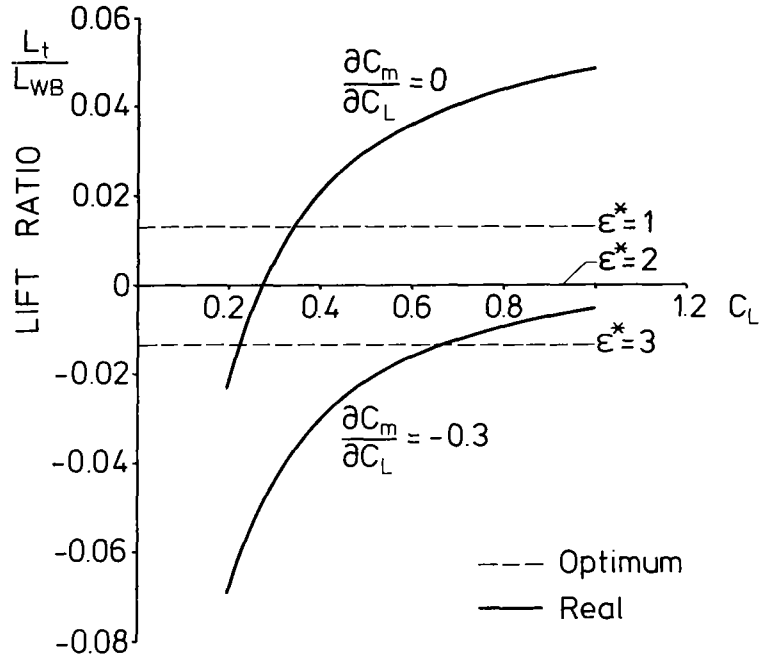

Fig. 2: Lift ratio between wing and tail

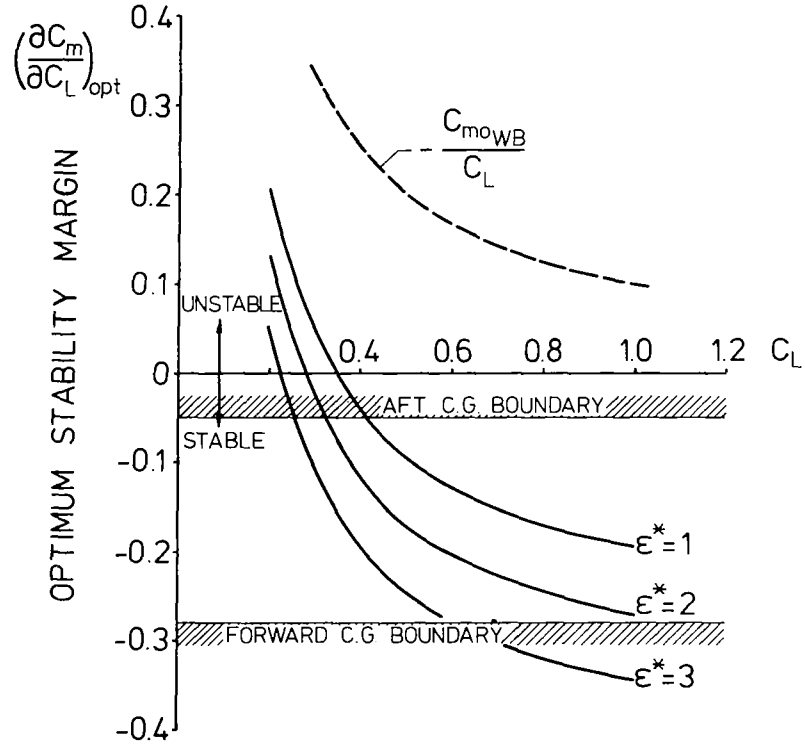

Fig. 3: Optimum stability margin

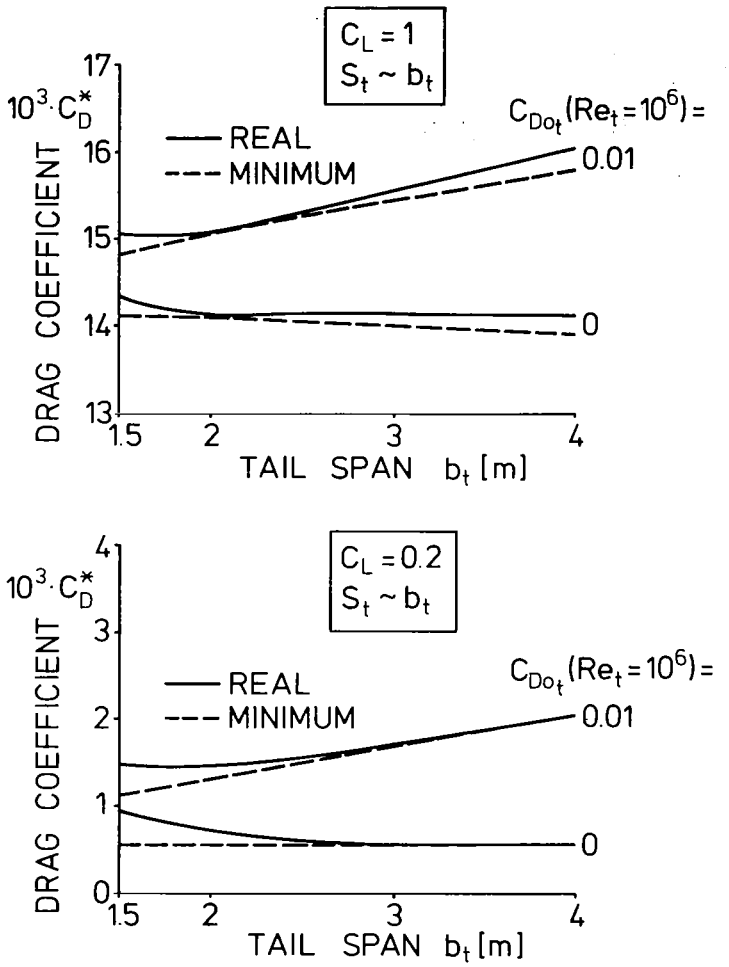

Fig. 4: Variation of tail span and area

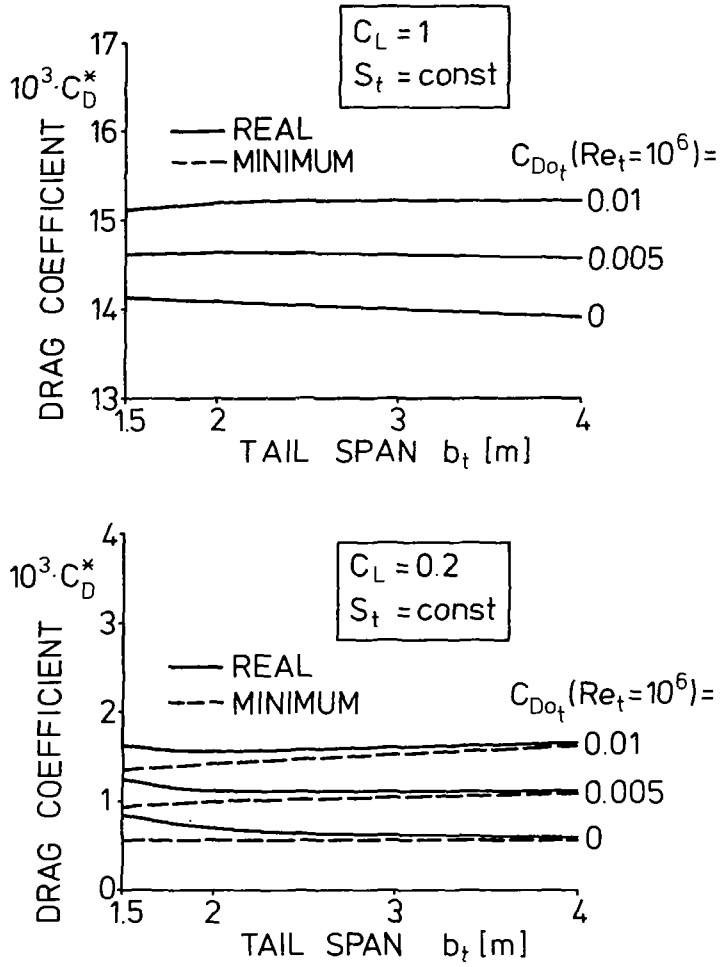

Fig. 5: Variation of tail span, tail area = const.

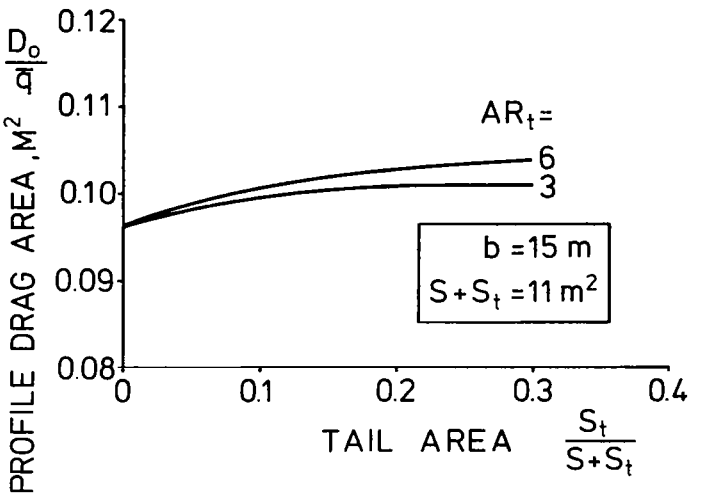

Fig. 6: Profile drag area versus tail area

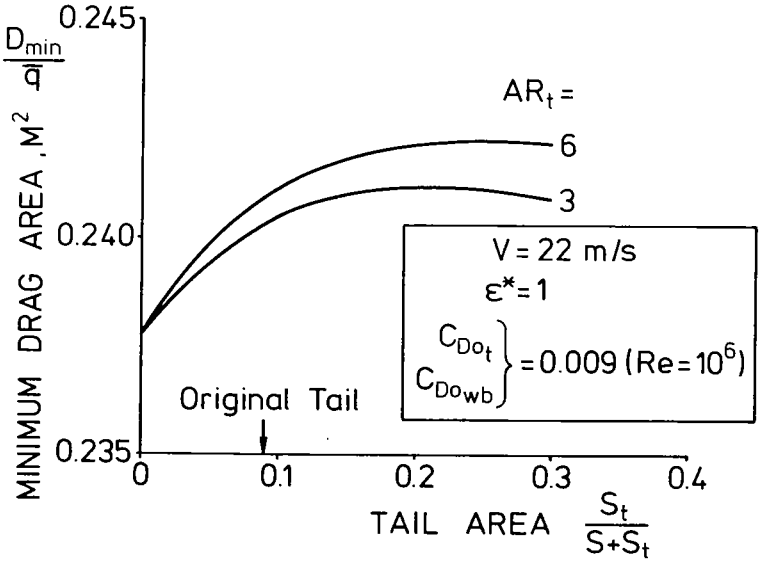

Fig. 7: Minimum drag area versus tail area